Fabrication and Characterization of Polyoxometalate based Nano-hybrids: Evaluation of their role in Biological Activity

SHIVA ARUN[1], PRABHA BHARTIYA[2], AMREEN NAZ[2], SUDHEER RAI[2], S.S. NARVI[2], AND P.K. DUTTA[2*]

[1] *Department of Humanities and Applied Sciences, School of Management Sciences, Lucknow-226501, India*

[2] *Department of Chemistry, Motilal Nehru National Institute of Technology Allahabad, Prayagraj-211004, India*

ABSTRACT

Polyoxometalates are a class of stable metal-oxide clusters with great molecular diversity having significant biological applications. Firstly, europium substituted polyoxometalate $K_4H[Eu(\alpha\text{-}SiW_{11}O_{39})\text{-}(H_2O)_2].17H_2O$ *(Eu-Si-POM) was synthesized and Eu-Si-POM was encapsulated into biocompatible chitosan (CS), through ionotropic gelation technique thus synthesizing a nano-hybrid (CS-Eu-Si-POM). CS-Eu-Si-POM retained the fluorescence property even after encapsulation. The nano-hybrid CS-Eu-Si-POM was characterized using FT-IR, UV-Vis spectra, fluorescence spectra, scanning electron microscopy (SEM), atomic force microscopy (AFM) and dynamic light scattering (DLS). Eu-Si-POM was further characterized by inductively coupled plasma (ICP) technique. These characterization techniques reveal the successful encapsulation of Eu-Si-POM within CS matrix by electrostatic interaction between cationic CS and anionic Eu-Si-POM. CS-Eu-Si-POM was applied as a fluorescent probe in A549 cell lines fluorescence imaging. The antibacterial activity of (CS-Eu-Si-POM), CS and Eu-Si-POM have been tested against bacterial strains of* B. subtilis *gram (+) ve and* P. *aeruginosa gram (-) ve. The (CS-Eu-Si-POM) showed enhanced antibacterial activity as compared to bare POM and CS.*

KEY WORDS : *Chitosan, Polyoxometalate, Antibacterial assay, Imaging reagent*

J. Polym. Mater. Vol. **35,** No. 4, 2018, 475-484

Correspondence author e-mail: pkd@mnnit.ac.in
DOI : https://doi.org/10.32381/JPM.2018.35.04.6

1. INTRODUCTION

Polyoxometalates (POMs) are a prominent class of anionic oxo-clusters having transition metal (mostly W, Mo, V) in their higher oxidation states with diversity in composition and size. In recent year polyoxometalates (POMs) have regained considerable interest due to their promising antibacterial[1-2], antiviral[3] and anticancer activities[4]. The strong redox ability of POMs can be utilized for building organic-inorganic hybrid materials possessing luminescence properties[5]. Rare earth substituted POMs like europium containing polyanions have fascinated researchers due to their excellent luminescence properties[6-9]. The luminescence properties of rare earth substituted POMs can be utilized for laser devices, bio-analysis and medical diagnosis[10-12]. Encapsulation of bioactive rare earth substituted POMs into biocompatible polymers like chitosan (CS), provide new avenues for development of drugs[13-18] having high potential bioactivity[19] with reduced toxicity, effective bio-distribution and greater stability at different pH[20].

Chitosan (CS) is obtained by N-deacetylation of chitin which is found lavishly in exoskeleton of shrimps and shells of crustacean. It is the second most abundant polysaccharide found in nature after cellulose[21]. CS is a muco-adhesive, polycationic biopolymer composed of N-acetyl glucosamine and glucosamine linked together by β 1-4 glucosidic bonds as repeating unit. Diverse CS derivatives can be produced by modifying the free amine and hydroxyl groups of CS[22]. It also offers a high degree of biocompatibility and activity including antifungal, insecticidal and wound healing properties[23]. CS has been widely explored as a carrier for the delivery of various genes, drugs and vaccines. The combination of rare earth substituted POMs with CS or its derivatives provides multiple advantages, like imaging reagents, passive drug targeting, prolonged drug circulation time and reduction of side effects[24].

In the present communication we have synthesized rare earth metalated POM $K_4H[Eu(\alpha\text{-}SiW_{11}O_{39})(H_2O)_2].17H_2O$ [Eu-Si-POM] according to the reported literature[25]. The synthesized [Eu-Si-POM] was encapsulated in CS, thus forming an organic-inorganic hybrid [CS-Eu-Si-POM]. The attractive properties of each component of the hybrid material motivated us to merge them and make a possibly more operative material[7].

2. EXPERIMENTAL

2.1 Materials and Characterization Techniques

Chitosan (low molecular weight), silicotungstic acid $H_4[SiW_{12}O_{40}].xH_2O$, Eu_2O_3 and HNO_3 anhydrous were purchased from Sigma Aldrich. Acetic acid, potassium bicarbonate, ethanol were purchased from CDH of A.R. grade. Nutrient agar and Nutrient broth were purchased from Titan Biotech Ltd. Rajasthan, India. The test strain *B. subtilis*, gram (+) ve. bacteria and P. aeruginosa gram (-) ve. bacteria were obtained from IMTECH, Chandigarh, India. FT-IR spectra were recorded in the range of wave number 4000–400 cm^{-1} using KBr disks with Perkin Elmer spectrophotometer. Nova Nano FE-SEM 450 (FEI) is coupled to EDAX detector for measuring the elemental composition of materials. UV–visible spectra were obtained with Shimadzu UV-2450. Particle size measurement was accomplished by Dynamic light scattering (DLS) technique using Nano Microtrac total solution in the particle characterization software. ICP-AES analysis was performed by SPECTRO Analytical Instruments GmbH- ARCOS, Simultaneous ICP Spectrometer.

Fluorescence properties were assessed by Perkin Elmer LS-45 Fluorescence Spectrometer. Fluorescence spectra were recorded for excitation wavelength of 395 nm.

2.2.1. Preparation of $K_4H[Eu(\alpha\text{-}SiW_{11}O_{39})(H_2O)_2].17H_2O$:

Rare earth metalated POM $K_4H[Eu(\alpha\text{-}SiW_{11}O_{39})(H_2O)_2].17H_2O$ [Eu-Si-POM] was synthesized according to the procedure reported by Y. Shen et al[25]. The molecular formula of Eu-Si-POM was confirmed by inductively coupled plasma atomic emission spectroscopy (ICP-AES). The calculated and found percent of Eu-Si-POM by ICP-AES data having chemical formula ($K_4H[Eu(\alpha\text{-}SiW_{11}O_{39})(H_2O)_2].17H_2O$; Calculated % Eu,4.52; K,4.72; Si,0.87; W,60.80 found% Co, 4.48; K,4.78; Si,0.90; W,60.85. Under UV excitation the Eu-Si-POM shows red fluorescence.

2.2.2. Preparation of CS-Eu-Si-POM nano-hybrid:

To prepare the nano-hybrid of Eu-Si-POM with chitosan, the polymer was dissolved in 2% v/v acetic acid to give concentrations of 0.50% w/v. The solution was filtered to remove any suspended particles (Solution1). pH of above solution was maintained at 5.0 with NaOH. 0.1 gm of Eu-Si-POM was dissolved in minimum amount of milli-Q water (Solution 2). Under the controlled sonication, Solution 2 was added to Solution 1 drop-wise for 4 minutes forming a stable colloidal suspension of CS-Eu-Si-POM nano-hybrid. CS-Eu-Si-POM nano-hybrid was separated by centrifugation which was run for 20 min at 20,000rpm.

3. Evaluation of hybrid material

3.1. Antibacterial assessment

Antimicrobial study of europium substituted POM $[Eu(\alpha\text{-}SiW_{11}O_{39})(H_2O)_2]^{4-}$, CS and their CS-Eu-Si-POM nano-hybrid were tested against two bacterial strains of *B. subtilis* gram (+) ve and *P. aeruginosa* gram (-) ve. By using agar disc diffusion method antimicrobial test was performed[26]. In brief, nutrient agar media (28 g/L in water) and nutrient broth (13 g/L in water) were prepared. The nutrient agar media was then poured into autoclaved petri dishes. The active broth culture of each bacterial strain was spread on nutrient agar plates. In inoculated agar plates were treated with 50 µg of Eu-Si-POM, CS and nano-hybrid in 100 µl of aqueous solution and put in wells (10 mm) with control (water). The incubation was continued for 14 h at 37°C, when finally the zone of inhibition around disc was measured in (mm) to determine the antibacterial efficacy.

3.2. Cell Imaging

In order to assess the potential biological application and usability of CS-Eu-Si-POM nano-hybrid in the cell, the A549 cell line (human lung carcinoma cell) were incubated with CS-Eu-Si-POM nano-hybrid (10 mg/mL) at 37 °C with 5% CO_2 for 24h[27].

4. RESULTS AND DISCUSSION

4.1.1. UV-Visible Spectra

The UV-Vis spectra of Eu metalated POM obtained were in accordance with the reported literature [25] thus confirming the formation of Eu-Si-POM (fig. 1 a). UV-Vis spectra of CS-Eu-Si-POM nano-hybrid display no shift in peak position, only the intensity of peaks in nano-hybrid decreased (fig. 1b).

4.1.2. FT-IR spectra

FT-IR (cm^{-1}) peaks of Eu-Si-POM and CS in fig. 2 (a,b) were in accordance with reported in literatures. The characteristic peak of CS at 1636 corresponding to N-H bending vibration (amines) and the peak at 1072 is due to the bridge oxygen (C-O-C) stretching vibration[28]. Similarly, in Eu-Si-POM the peak at 1003 and 950 is due to Eu-O oscillation[25]. The peaks at 725 (ν_{asym}W-O-W), 795 ((ν_{asym}W-O-W), 858 (ν_{asym}W-O-W), 896 (ν_{asym} W-O-W), 950 (ν_{asym} W=O)[29]. The characteristic FT-IR peaks of CS and Eu-Si-POM were present in CS-Eu-Si-POM nano-hybrid (fig. 2c) with minor shifts thus indicating the encapsulation of Eu-Si-POM into CS.

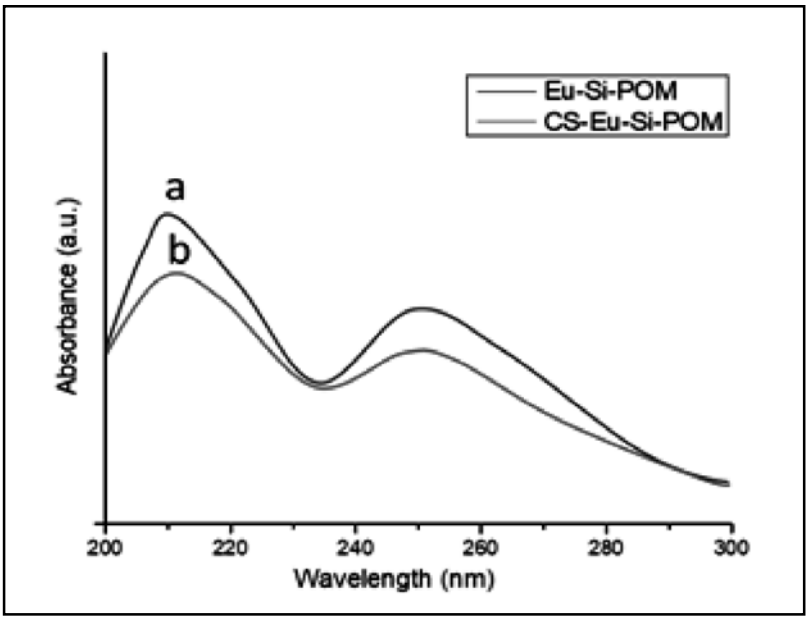

Fig. 1. UV-Vis of (a) Eu-Si-POM (b) CS-Eu-Si-POM nano-hybrid

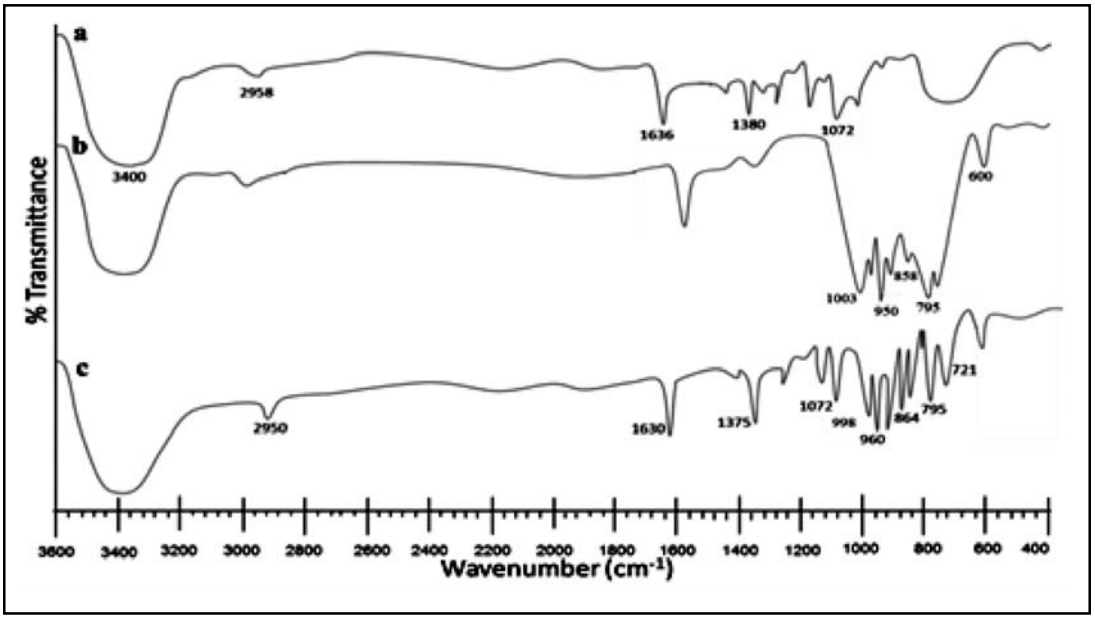

Fig. 2. FT-IR (cm^{-1}) of (a) Eu-Si-POM (b) CS (c) CS-Eu-Si-POM nano-hybrid

4.1.3. SEM Image

The SEM image (fig. 3) of CS-Eu-Si-POM nano-hybrid shows monodispersed nanoparticles with spherical morphology.

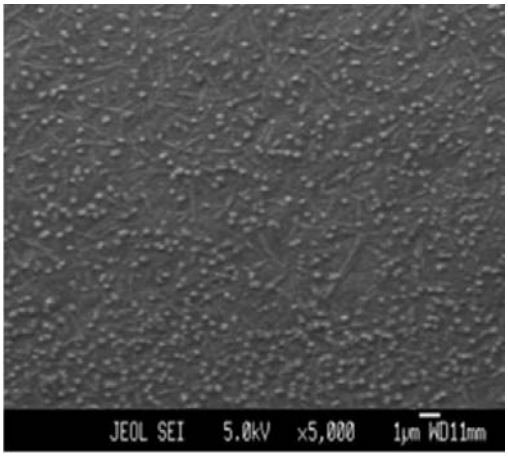

Fig. 3. SEM image of CS-Eu-Si-POM nano-hybrid

4.1.4. DLS histogram

DLS study shows the synthesized of CS-Eu-Si-POM nano-hybrid size ranged about 100-130 nm with a low polydispersity index.

4.1.5. Photoluminescence Property

The luminescence emission spectra of [Eu-Si-POM] and organic-inorganic hybrid [CS-Eu-Si-POM], excited at 395 nm, respectively, are given in Fig. 5. Each of the luminescence spectra for the [Eu-Si-POM] and [CS-Eu-Si-POM] shows five characteristic emission peaks. These peaks are assigned to five energy level transitions from $^5D_0$ metastable state to terminal levels, respectively: ^7Fj (j = 0–4) transitions. More clearly, the luminescence intensity of the induced electronic dipolar transition $^5D_0 \rightarrow {}^7F_2$ and magnetic transition $^5D_0 \rightarrow {}^7F_1$ are predominant transitions in the two states. For the [Eu-Si-POM] complexes, the transition $^5D_0 \rightarrow {}^7F_2$ peak splits into two peaks at 615 and 619 nm, and the secondarily intense transition $^5D_0 \rightarrow {}^7F_1$ appears at 589 and 594 nm[30]. The peak at 581 nm is ascribed to the $^5D_0 \rightarrow {}^7F_0$, while the peaks at 652 and 702 nm correspond to $^5D_0 \rightarrow {}^7F_3$ and $^5D_0 \rightarrow {}^7F_4$ transitions, respectively. Compared with the spectrum of the [Eu-Si-POM], the spectrum of the organic-inorganic hybrid [CS-Eu-Si-POM] shows some

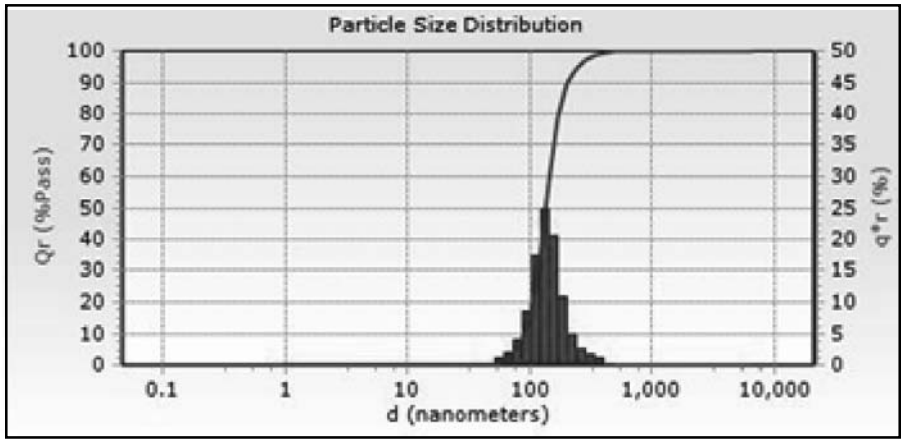

Fig. 4. SEM image of CS-Eu-Si-POM nano-hybrid

differences in shapes, position, and splitting lines. The $^5D_0 \rightarrow {}^7F_1$ emission transition occurs at 588 nm and the peak at 611 nm is $^5D_0 \rightarrow {}^7F_2$, and no splitting is observed. The relative intensity between the two predominant transitions also varies. It is well known that the hypersensitive emission $^5D_0 \rightarrow {}^7F_2$ is expected to be more sensitive to the ionic environment in terms of shift in peak position as well as the relative intensity. The ratio between the electronic dipolar transition $^5D_0 \rightarrow {}^7F_2$ intensity and magnetic dipolar transition $^5D_0 \rightarrow {}^7F_1$ intensity is used as the measure of rare earth site symmetry [31]. The intensity ratio of $^5D_0 \rightarrow {}^7F_2/{}^5D_0 \rightarrow {}^7F_1$ for the bare POM and the hybrid POM is about 1.48 and 1.14, respectively. The fact suggests a more asymmetrical environment occupied by the Eu^{3+} in the hybrid POM than in bare POM. The transitions between the resonance energy levels of Eu^{3+} may be altered when the site symmetry of Eu^{3+} is changed. The changes are possibly due to the formation of hybrids between the polyanions and the polymer.

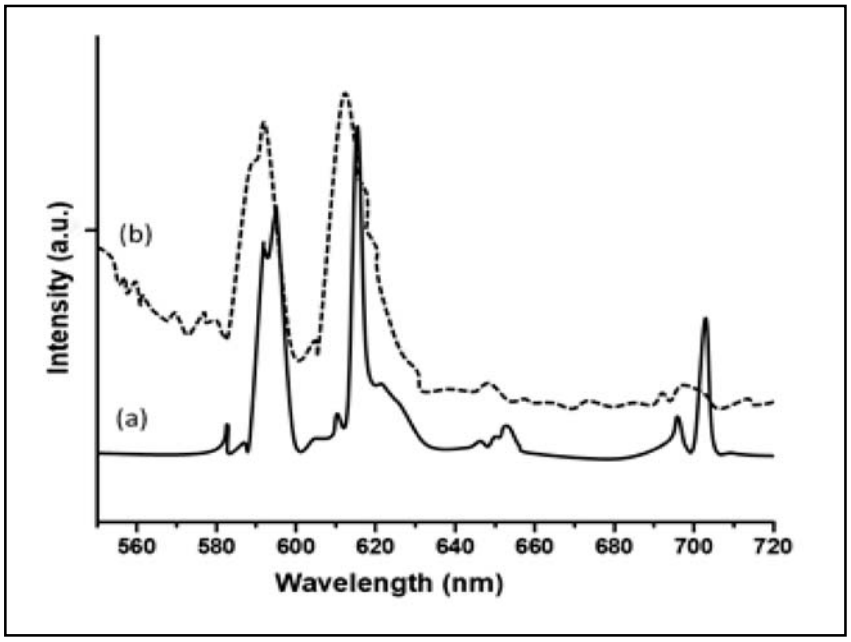

Fig. 5. Emission spectra of (a) Eu-Si-POM and (b)CS-Eu-Si-POM nano-hybrid

4.1.6. Cell Imaging

As can be seen in Fig. 6, under a 530 nm laser excitation, the A549 cells treated with CS-Eu-Si-POM nano-hybrid for an incubation period of 4 h emit red fluorescence primarily from the cytoplasm, suggesting that CS-Eu-Si-POM nano-hybrid could be efficiently uptaken by the A549 cells and thereby possess great promise in serving as effective optical nanoprobes for bio-imaging purpose. Meanwhile, bare POM treated cell lines shows less intense fluorescence in cytoplasm region for same

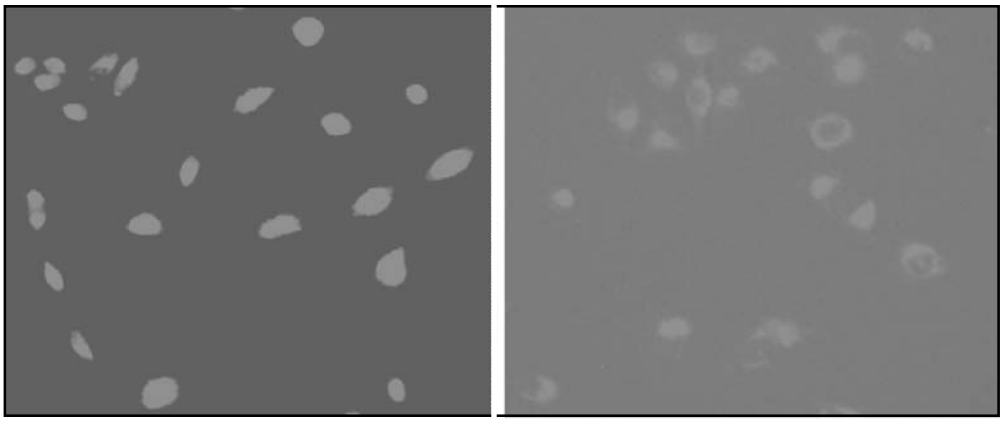

Fig. 6. Fluorescence images of A549 cells treated with CS-Eu-Si-POM nano-hybrid and Eu-Si-POM

incubation period attributing to low cell penetration ability of bare POM.

4.1.7.Antibacterial assessment

The antibacterial properties of Eu-Si-POM, CS and their nano-hybrid have been tested against two bacterial strains *B. subtilis* (gram + ve) and *P. aeruginosa* (gram – ve), the effect of nano-composite and individual component (inhibitory zone) data are tabulated in (Table 1). Eu-Si-POM have shown significant growth inhibitory effects on gram (+) ve but less significant on gram (-) ve bacteria. The inhibitory effects of CS-Eu-POM nanohybrid against *B. subtilis* and *P. aeruginosa* bacteria are shown in (Fig. 7). Chitosan itself has antibacterial activity and most acceptable antimicrobial mechanism of chitosan is due to the presence of charged groups, which form by protonation of amino groups [NH_3^+] in their polymer chain and which form ionic interactions with bacteria wall constituents. This interface may be leading to the hydrolysis of the peptidoglycans membrane in the microorganism wall, provoking the leakage of intracellular electrolytes, leading the bacterial to death. The data represent that CS-Eu-POM do show potential antimicrobial activity against both gram positive and negative. It is clear from the figure Eu-Si-POM not shown itself major antibacterial activity, whereas chitosan itself have potential antimicrobial activity. But when Eu-Si-POM is formed nano-hybrid with chitosan, then chitosan bio-activity got synergistically increased (Table 1).

Table 1. The measured values of inhibitory zone (mm) by antibacterial activities of Eu-Si-POM, chitosan and nanohybrid against *B. subtilis* (gram + ve) & *P. aeruginosa* (gram - ve) bacteria

Samples	Diameters of inhibitory zone (mm)	
	B. subtilis (gram + ve)	*P. aeruginosa* (gram –ve)
$[Eu(\alpha\text{-}SiW_{11}O_{39})(H_2O)_2]^{3-}$	23 ± 1	21 ± 1
Chitosan	36 ± 2	34 ± 1
CS-Eu-Si-POM Nano-hybrid	41 ± 1	37 ± 1

A possible explanation of this observation lies in the difference in composition of outer membrane of gram (+) ve and gram (-) ve bacteria. Gram (+) ve bacterial cell walls are rich in lipoproteins and phospholipids than gram (-) ve bacteria which might enhance the permeability of cobalt related compounds which is present in polyoxometalate complex [32]. Another argument in favor of above observation relates to the inherent defense mechanism adopted by the gram (-) ve bacteria owing to the presence of unique periplasmic space which is not present in gram (+) ve bacteria. The opposition of gram negative bacteria towards antibacterial agents lies in the presence of hydrophilic surface of their outer membrane which is rich in lipoproteins and lipopolysaccharide causing a barrier to the diffusion of antimicrobial agent.

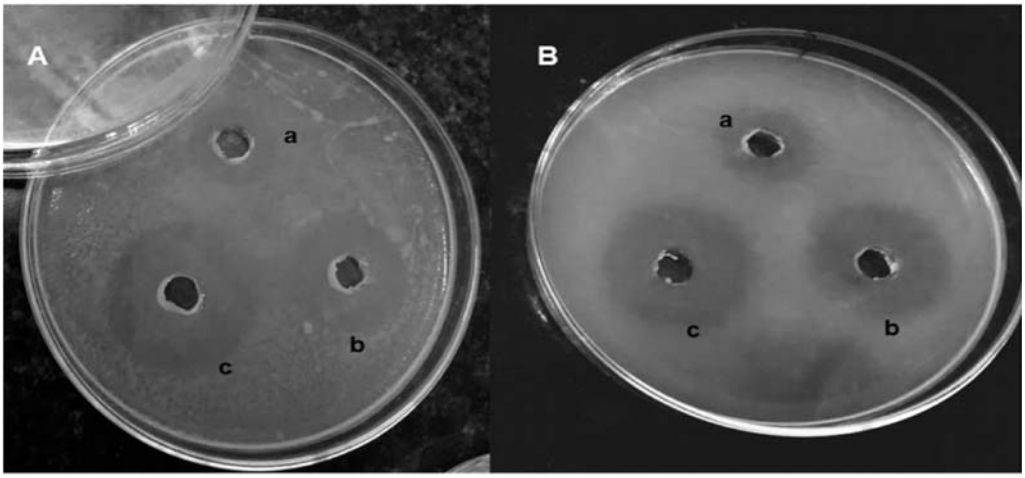

Fig. 7. Images of antibacterial effect (inhibitory zone) of $[Eu(\alpha\text{-}SiW_{11}O_{39})(H_2O)_2]^{3-}$ (a) chitosan (b) and their CS-Eu-Si-POM nano-hybrid (c) against gram (+) ve bacteria *B. subtilis* (121, A) & gram (-) bacteria *P. aeruginosa* (1688, B).

We conclude that the enhanced antimicrobial properties, shown by the CoSLPOM-CS nanocomplex are largely due to hydrophobicity, lipophilicity and capability of this compound to bind with proteins at acidic pH.

6. CONCLUSIONS

Eu-Si-POM was encapsulated into CS to synthesize nano-hybrid. The Formation of europium metalated POM and nanohybrid was confirmed by relevant techniques. Eu-Si-POM exhibits intense fluorescence and its nano-hybrid retain the fluorescence property even after encapsulation. CS-Eu-Si-POM act as an imaging reagent in A549 cell lines. Antimicrobial activity of Eu-Si-POM, chitosan and their nano-hybrid were tested against two bacterial strains of B. subtilis gram (+) ve and P. aeruginosa gram (-) ve. The nano-hybrid showed enhanced antibacterial activity as compared to chitosan and Eu-Si-POM.

REFERENCES

1. A. Maalaoui, A. Hajsalem, N. Ratel-Ramond, and S. Akriche, *Journal of Cluster Science,* vol. 25, no. 6, 1525–1539, 2014.
2. H. S. Shah, R. Al-Oweini, A. Haider, U. Kortz, and J. Iqbal, *Toxicology Reports,* vol. 1, 341–352, 2014.
3. T. Rhule, C. L. Hill, D. A. Judd, and R. F. Schinazi, Chemical Reviews, vol. 98, no. 1, 327–357, 1998.
4. J. T. Rhule, C. L. Hill, D. A. Judd, R. F. Schinazi, *Chem. Rev.,* 98 (1998) 327 – 357.
5. Y. Shen, J. Peng, C. Chen, D. Chen, H. Zhang and C. Meng, "Synthesis and Characterization of Fluorescent Polyoxometalate Nano-/ Microrods," 65b, 603-606, 2014.
6. J. Wang, H. S. Wang, L. S. Fu, F.Y. Liu and H. J. Zhang, "Thin Solid Films", 415, 242–247, 2002.
7. R. D. Peacock and T. J. R.Weakley, *J. Chem. Soc.* (A) 11, 1836 – 1839, 1971.
8. B. S. Bassil, M. H. Dickman, B.V. D. Kammer, U. Kortz, *Inorg. Chem.,* 46, 2452 – 2458, 2007.
9. I. Creaser, M. C. Heckel, R. J. Neitz, M. T. Pope, *Inorg. Chem.,* 32, 1573 – 1578, 1993.
10. J. Kido, H. Hayase, K. Hongawa, K. Nagai, K. Okuyama, *Appl. Phys. Lett.,* 65, 2124 –2126, 1994.
11. M. Li, P. R. Selvin, *J. Am. Chem. Soc.,* 117, 8132 –8138, 1995.
12. F. S. Richardon, *Chem. Rev.,* 82, 541 – 552, 1982.
13. L. Zhang, J. M. Chan, F. X. Gu, J.-W. Rhee, A. Z. Wang, A. F. Radovic-Moreno, F. Alexis, R. Langer and O. C. Farokhzad, *ACS nano,* 2 (2008) 1696-1702.
14. K. A. Whitehead, R. Langer and D. G. Anderson, *Nature reviews Drug discovery,* 8 (2009) 129-138.
15. N. Bertrand and J.-C. Leroux, *J. Controlled Release,* 161 (2012) 152-163.
16. V. M. Pandya, U. Kortz and S. A. Joshi, *Dalton Trans.,* 44 (2015) 58-61.
17. H. S. Shah, R. Al-Oweini, A. Haider, U. Kortz and J. Iqbal, *Toxicol. Rep.,* 1 (2014) 341-352.
18. J. Zhou, P. Yin, X. Chen, L. Hu, T. Liu, *Chem.Comm.,* 51 (2015) 15982-15985.
19. (a) M. Bonchio, M. Carraro, G. Scorrano, E. Fontananova, E. Drioli, *Adv. Synth. Catal.,* 345 (2003) 1119 – 1126. (b) G. Geisberger, S. Paulus, M. Carraro, M. Bonchio, G.R. Patzke, *Chem. Eur. J.* 17 (2011) 4619–4625. (c) T. Meißner, R. Bergmann, J. Oswald, K. Rode, H. Stephan, W. Richter, H. Zänker, W. Kraus, F. Emmerling, G. Reck, *Transit. Met. Chem.* 31 (2006) 603–610.
20. F. Zhai, D. Li, C. Zhang, X. Wang, R. Li, *European Journal of Medicinal Chemistry,* 43 (2008) 1911-1917.
21. P. K. Dutta, J. Dutta, M. C. Chattopadhyaya, V. S. Tripathi, *J. Polym. Mater.,* 21 (2004) 321-333.
22. (a) A. Anitha, V. V. Divya Rani, R. Krishna, V. Sreeja, N. Selvamurugan, S. V. Nair, *Carbohydrate Polymers,* 78 (2009) 672–677; (b) R. Jayakumar, N. Nwe, S. Tokura, H. Tamura, *International Journal of Biological Macromolecules,* 40 (2007) 175–181.
23. (a) D. Archana, J. Dutta, P. K. Dutta, *International Journal of Biological Macromolecules,* 57 (2013) 193-203. (b) D. Archana, B. K. Singh, J. Dutta, P. K. Dutta, *International Journal of Biological Macromolecules,* 73 (2015) 49-57. (c) B. K. Singh, R. Sirohi, D. Archana, A. Jain P. K. Dutta, *International Journal of Polymeric Materials and Polymeric Biometarials,* 64 (2014) 242-252.
24. P. K. Dutta, J. Dutta, V. S. Tripathi, *J. Sci. Ind. Res.,* 63 (2004) 20–31.
25. Yan Shen, Jun Peng, Changyun Chen, Dan Chen, Huanqiu Zhang, and Cuili Meng, Synthesis and Characterization of Fluorescent Polyoxometalate Nano-/Microrods, 65(b) (2010) 603-606.
26. S. Tripathi, G. K. Mehrotra, P. K. Dutta, *Bull. Mater. Sci.,* 34 (2011) 29–35.

27. D. Menona, R. T. Thomas, S. Narayanan, S. Maya, R. Jayakumar, F. Hussain, V. K. Lakshmanan, S. V. Nair, *Carbohydrate Polymers*, 84 (2011) 887–893.

28. S. Saha, A. Ghosh, P. Mahato, S. Mishra, S. K. Mishra, E. Suresh, S. Das, A.Das, *Org. Lett.* 12 (2010) 3406–3409.

29. Z. Xin, J. Peng, T. Wang, B. Xue, Y. Kong, L. Li, E. Wang, Keggin POM *Inorganic Chemistry,* 45 (2006) 8856-8858.

30. G. Blasse, G.J. Dirksen, *J. Inorg. Nucl. Chem.* 43 (1981) 2847-53.

31. M. Dejneka, E. Snitzer, R.E. Riman, *J. Non-Cryst. Solids,* 202 (1996) 23-24.

32. G. Fiorani, O. Saoncella, P. Kaner, S. A. Altinkaya, A. Figoli, M. Bonchio, M. Carraro, *J. Clust. Sci.,* 25 (2014) 839-854.

Received: 16-01-2019

Accepted: 17-02-2019